

An Experiment on Thermal Damage Prevention via Power Control in Bipolar Electrosurgical Unit

Ali Idham Abdullah, Azli yahya, Mohammad Rava, Tan Tin Swee, Norhalimah Idris

Abstract — This article presents a model of the ESG system for a Thermal control of bipolar electrosurgical device which accurately predicts the thermal spread rate for particular electrodes and tissue. A value for the tissue cutting and coagulation has been identified based on the analysis carried out on the experimental data and compared with the simulation result from the model using the Matlab/Simulink simulation tool. The ESG controller is designed based on the Microcontroller.

Keywords— Bipolar, Thermal Damage, Thermal Monitoring, Thermal Control, PID, Electrosurgical,

I. INTRODUCTION

Electrosurgery has become a common form of modern surgery, and it has been widely used practice for many procedures that involve hemostasis status [1]. Currently, in the clinical Electrosurgery process, there is no control method in which can reactively regulate the temperature. This is mainly due to the fact that everything is pre-set, and if the surgeon intends on preventing the damage to the tissue, he has to perform it manually, by visual inspection, which is highly inaccurate and prone to error [2]. This issue is further compounded by the fact that there are multiple tissue types, and damage is registered differently depending on the type. Thus, a qualitative approach has been undertaken that takes notes of the guidelines and experience that would regulate the Electrosurgery [3]. This Paper discusses the process for simulation of Electrosurgery. We present a new self-thermal regulated with high-frequency converter topology which eliminates these unwanted responses by regulating the power. The simulation is done by using MATLAB/Simulink and simulation results are presented. This paper discusses the process for simulation of thermal control system and converters for ESU. Firstly, a discussion on power control system in ESU, Secondly, thermal control system are design and implementation. Thirdly, Flyback converter topology and Inverter are presented a calculation on components value is conducted based on required specification development of mathematical equation for converter behaviour model.

Manuscript published on 30 June 2019.

* Correspondence Author (s)

Ali Idham Abdullah, Faculty of Biomedical Engineering, Universiti Teknologi Malaysia (UTM), Skudai, Johor, Malaysia

Azli yahya, Faculty of Electrical engineering, Universiti Teknologi Malaysia (UTM), Skudai, Johor, Malaysia

Mohammad Rava, Faculty of Computing, Universiti Teknologi Malaysia (UTM), Skudai, Johor, Malaysia

Tan Tin Swee, Faculty of Biomedical Engineering, Universiti Teknologi Malaysia (UTM), Skudai, Johor, Malaysia

Norhalimah Idris, Faculty of Management, Universiti Teknologi Malaysia (UTM), Skudai, Johor, Malaysia

© The Authors. Published by Blue Eyes Intelligence Engineering and Sciences Publication (BEIESP). This is an [open access](https://creativecommons.org/licenses/by-nc-nd/4.0/) article under the CC-BY-NC-ND license [http://creativecommons.org/licenses/by-nc-nd/4.0/](https://creativecommons.org/licenses/by-nc-nd/4.0/)

lastly, the simulation result for each model The dynamic behaviour and control design of ESG. A mathematical equation for calculating the electronics components value is presented. A state representation of generator which include converter and inverter with its suitable control approach is identified from the theoretical and evaluated using SIMULINK/MATLAB simulations. An output voltage response shows the simulated HF inverter and converter validate the theoretical calculation. From the simulation, the desired output voltage can be observed when lead compensation network is implemented, thus allow for practical implementation. The block diagram used in order to simulate the mode is illustrated in Figure 1.

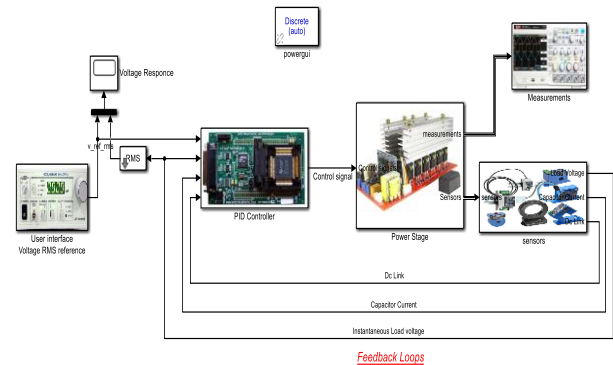


Figure 1: The block diagram of new model ESG

Table 1. which is the design table and the specification of the electrosurgical generator under new design for the thermal control and dc converter as show in the table the specification and design for new simulation results.

Table 1: Summary Design Specifications

Parameter	Specification
Input Voltage Range	80 to 120 VDC
Output Frequency at 50 Ohm	100kHz
Max output power	112 Watts at 20 Ohms
Output power derating	13 Watts at 500 Ohms
Output Load Impedance	20 to 500 Ohms
Max output voltage at no load	600 Volts peak to peak
Max output current at full load	2.5A RMS
Efficiency	>90% at full power

II. TEMPERATURE CONTROLLER SYSTEM

A temperature controller is used in any situation in which a specific constant temperature needs to be maintained. The object to be temperature regulated may need to be cooled or heated or both to sustain a constant temperature (setpoint); this control needs to be achieved irrespective of changes within the surrounding environment [4].



An Experiment on Thermal Damage Prevention via Power Control in Bipolar Electrosurgical Unit

Open loop and closed loop control represent the two basic forms of temperature control, of which open loop is the simplest. This type is similar to a car's heating system; it provides continuous heating/cooling but is unable to take any account of the actual temperature output. On the other hand, in the closed loop type of control the output temperature is monitored constantly and adjusted appropriately to keep the output consistent. This type of regulation is superior to that of open loop control. The output signal of closed loop control is always monitored and the information is fed back to modulate the control process [6]. Closed loop control is akin to internal control. If the temperature is set to 75°, automatic adjustments are made providing heat on cold days, or cooling on warm days, to keep the temperature at the desired 75° setting. Figure 2 illustrates the closed loop block diagram.

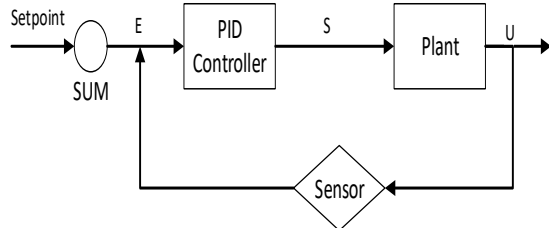


Figure 2: Closed loop control block diagram

Temperature controllers are apparatus that maintain the temperature at a particular desired value. Household thermostats, such as hot water heaters, are an example of a simple temperature controller. In this example, a thermostat regulates the temperature of the water, keeping it at the specific, desired temperature. Ovens also use temperature controllers [4]. In setting the temperature of an oven, the actual temperature inside the oven is detected by the controller; should the internal temperature drop below the setpoint, a signal is initiated, activating the heater to re-establish the desired temperature. Refrigerators also use thermostats, with the controller reducing the temperature should it rise too high.

A. Parts of a Temperature Controller for ESG

There are a number of components that are consistent across all controllers. For example, inputs, which measure a variable in the process that is being regulated; in temperature control, the variable is measured by the input is the temperature. Inputs Temperature controllers can have several types of inputs. There can be variation in the sort of input sensor and signal required according to the controlled process. Thermocouples, resistive thermal devices (RTD's) and linear inputs such as mV and mA, are common examples of input sensors. There are several types of standardised thermocouple, which include, but are not limited to B, J, K, L, R, S, and T types. RTDs can also be accepted as a temperature sensing input by controllers. In a closed loop system, ADC can convert the measured temperature to a voltage value, which is then used by a PID controller as a voltage reference. Table 4.1 below depicts the different types of sensors and their conversion range [7]. Due to more number of external components and complexity of circuit to provide isolation and regulation of output voltage ESG, the modern science continuously looks for the best solution for the size and simplicity of ESG. Simplicity in design, small design, isolation and perfectly regulated output cannot be obtained in a single design of generators. The Figure 3 gives the block diagram of electrosurgical generator and [8].

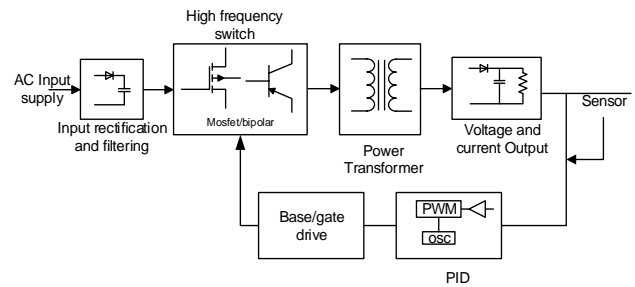


Figure 3 Block diagram of a ESG.

B. Thermal Control System Model

Using the sensors, the temperature can be read from the electrode. So now that, to control the power applied to the heating element with power circuit. Figure 4 depicts a circuit design that includes sensors to read the temperature, ADC and controller. The PID algorithm is already uploaded to this controller. We read the temperature, calculated the error, summed the PID values and created a PWM signal on a digital pin D3, which was applied to the MOSFET. The desired temperature was set at variable values, for example, 35°C, 65°C, 80°C and 100°C, and the LCD was used to print the set value and the real temperature. Figure 4 shows the result of the control. For this example, we set a variable setpoint of 100°C; then as in the past example, we read the thermocouple real-temperature value. Three constants were used to calculate the PID sum. Depending on that value, we created a PWM signal on pin D3 and applied it to the MOSFET gate using a BJT driver [18]. As the Figure 4 demonstrates, the temperature stays at the desired value. However, to achieve this result involved trying multiple PID constants, starting with I and D values equalling 0; these values were then slowly increased until good results were generated. Here on my oscilloscope, I have the PWM signal of the MOSFET connected. Because the primary concern is the actual implementation of this control, reducing the number of mathematical operations is useful. The current control loop can be simplified, due the value ascribed to the fictitious input current $i_0 \beta$ (8), as follow[19]. Figure 4 shows the proposed system implemented on Matlab Simulink. Dimensioning components and controllers' parameters are done in table 2. The controller section consists of thermal controller system and ADC then the processing. In our controller, the error fed to controller pin of system. In voltage mode controller, Vref and Vout are matched and specified to PID to reduce fault between them. Output is converter to PWM pulse by comparing with HF carrier [20]. There are three modes of operation namely current limiting mode, voltage limiting mode, power mode. The fig below show shows the output signal of the inverter before and after filtering.

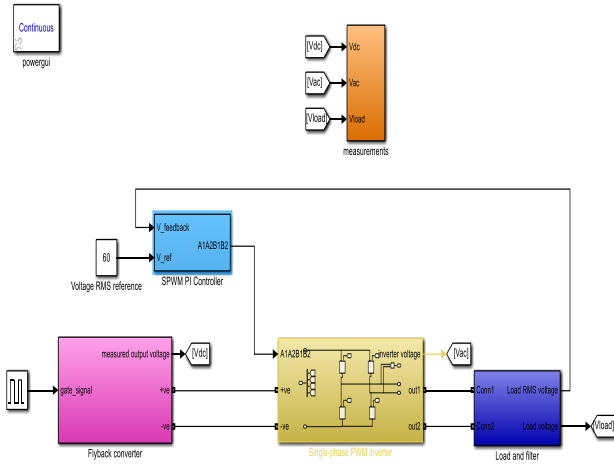


Figure 4: Controller System

Table 2 Controller Parameters

Control strategy	Parameters values
PID Parameters	$K_p=0.03;$ $K_I=0.5;$ $K_d=0.001.$

Simulation results are shown in part to validate the good behaviour of the system, using Matlab Simulink as environment, in cases of input temperature change load change and reference change [21]. shows the parameters used in the simulation model of the flyback system. The proposed flyback SMPS convert input DC power supply, ranging from 340 V to 100 V to DC output voltage with other circuit components parameter value fix [22]. Figure 4 shows the top-level system model of flyback SMPS which consist of constant input voltage, constant duty-cycle command, pulse-width modulator and a load modelled as a resistor. An open loop simulation of the flyback converter in MATLAB was performed; Figure 5 presents the result of that and the output voltage and waveform. As the waveform shows, the value of the output voltage and the calculated value are consistent.



Figure 5: Output waveform of close loop PI controller

The most effective and commonly applied control strategy in industry is the closed loop PID controller. The Figure 6 depicts the closed loop Simulink model with PID controller; this model eliminates the error of open loop converter. Using a continuous control using PID controller, results in a smooth curve in the voltage output waveform graph, and an absence in voltage oscillations as the error is eliminated fig (4.15).

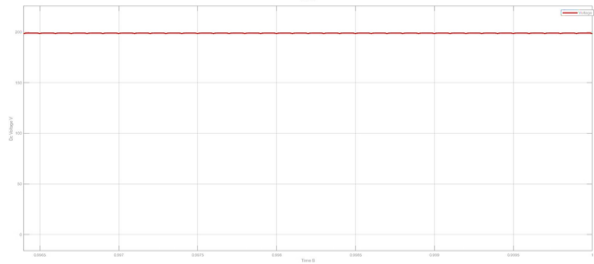


Figure 6: Output waveform of close loop PID controller

High voltage can be generated at the output of the inverter without switching losses across inverter switches. MOSFETS are used as switching device in HF transformer. It provides a three level output [23]. The circuit diagram and switching pattern is as shown in Fig 4.18. It consists of four modes. In mode 1, S1 and S4 will conduct. So the output voltage developed will be positive. In mode 2, S1 will be on but S4 will be turned off and S3 will conduct 90 degrees after S1 starts conducting. Then the output will be zero. Mode 3 will begin when S1 get turned off. S3 and S2 will conduct during this instant and output will be negative. In mode 4, S2 and S4 will be on and output will be zero. After mode 4 the same cycle will be again repeated [24]. The output voltage waveform is as shown in Fig 4.17.

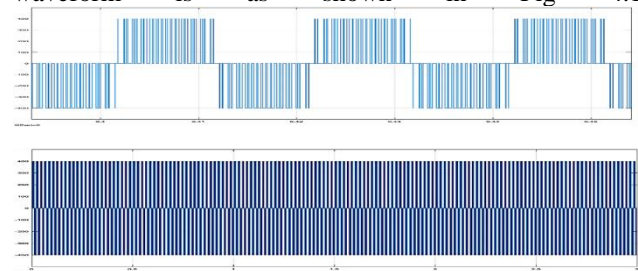


Figure 7: Output voltage graph for dc to Ac after filter

C. Open loop Thermal control system simulation Result

In the present section, the experimental arrangement described in Chapter 5 is used to compare the temperature waveforms obtained from the prototype with those simulated for a closed and open loop system. A voltmeter is used to measure the output voltage for skin and load resistances in the range 100 – 3000 Ω. The simulated open loop system (Figure 8) produces a plot of the output temperature as a solid blue line (Figure 9) The component tolerances and open loop response lead to a slightly lower amplitude for the simulation results relative to the setpoint. The results indicate that the setpoint varies with time and is not achieved in two cases. With an error of 1 – 3%, the results are in close agreement with the anticipated output. The analysis and design performance is completely proven by comparison of the simulated and experimental results.

An Experiment on Thermal Damage Prevention via Power Control in Bipolar Electrosurgical Unit

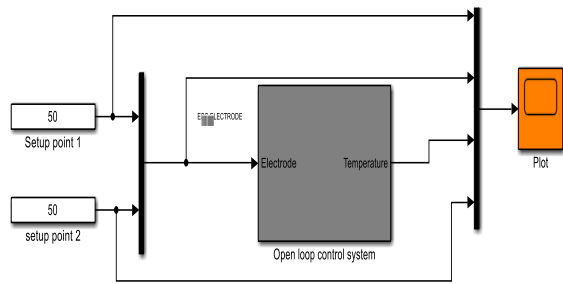


Figure 8: Open Loop thermal control system with two set point

In the Figure 9 the system was tested at two different setpoint and the response of the open loop control for each one as it shows clearly was at 50 C the of the system was did not reach the setpoint till take long time and the signal was not stable swinging between up and down and also when we make the transition in the setpoint to be 75C take longer time that what we expected to reach the setpoint which can be effected the system performance with error more than 1-3%.

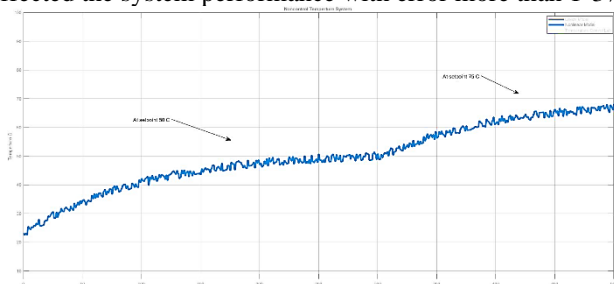


Figure 9 The result of open loop thermal control system at two setpoint 50C and 75 C.

D. Closed Loop Thermal control system Simulation result

The temperature control loop consists of the input and feedback whereby the user will set desired input value while electrode acts as the main process of the plant. Thermal sensor provides feedback to ensure that the desire actual temperature is achieved at the output. The temperature control loop will compensate the error between the set point (SP) and the process variable (PV) in order for this system to perform accordingly. heating element represents the heating element block while thermal sensor in the block is being represented by temperature sensor used in the project.

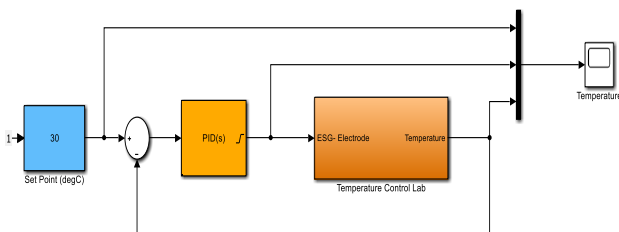


Figure 10 Close Loop thermal control system

Figure 10 shows the MATLAB monitoring on temperature sensors along with the ESG of the system when regulating at different degree Celsius. The real-time monitoring using MATLAB is able to provide accurate reading of the current process plant data read by the controller. Figure 11 shows real-time monitoring of the plant response when the controller tries to maintain at the set point of 50 degrees Celsius and 75 degrees Celsius. As show in the result and

comparison between the open loop and closed loop in the Figure 11 we noticed that the closed loop and can reach to setpoint faster and more accurate than the open loop.

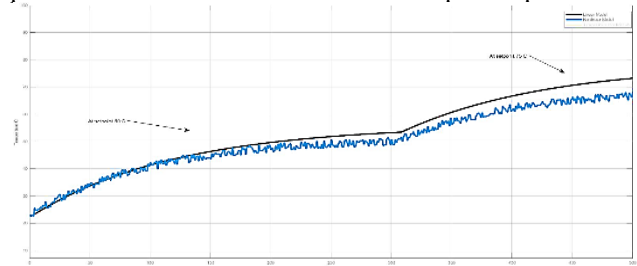


Figure 11 Close Loop thermal control system result

Demonstrate step changes in temperature set point and comment on the performance of the controller using the calculated constants. Tune the controller by adjusting the constants to improve performance. Comment on the difference between tuning constants and the improved tuning constants in terms of rise time, overshoot, decay ratio, heater fluctuations, or other relevant performance criteria. Tuning on a device that takes 10-20 minutes per test is much slower than running a PID controller in simulation. Once optimized PID tuning values are obtained, demonstrate the performance with the physical control lab.

E. Power Control unit simulation result

PID temperature controller will work. For any PID system, the final process needs to be defined; in this instance, it is the electrode's final temperature. To regulate this temperature, a feedback system using a K-type thermocouple capable of detecting the system's real temperature can be used. A setpoint, which here is the desired temperature, is required for this type of control. The system will use the output (error) to determine the difference between the desired value and the feedback, to ensure the electrode is precisely 80°C. To do this, power must be applied first, causing it to start heating up. As the temperature reaches the setpoint value of 80°C, the PID control is informed through feedback that the desired value has been attained; it accordingly reduces the power to the heating element. In the simulation below, our system will use a PWM signal, which will be applied to a high frequency inverter in an electrosurgical generator. This will regulate the voltage sent to the heating element inside the block. As Figure 12 shows, the PWM that is generated in response to the feedback signal is forwarded to the HF inverter to produce the voltage, which is proportional to temperature. It is evident that if the real temperature exceeds the setpoint, the power value needs to be reduced. In contrast, if the real temperature is below the setpoint, the power needs to be increased until the desired value is achieved. This is known as proportional control (P control); it produces temperature oscillations between particular values and is unable to achieve a stable state. To produce the required stability, a derivative or D control, is added. This form of control responds to the speed of the change in temperature. It is the sum of these three P, I and D parts that gives rise to a PID control. Our aim is to identify the correct constants for each element of the PID control.



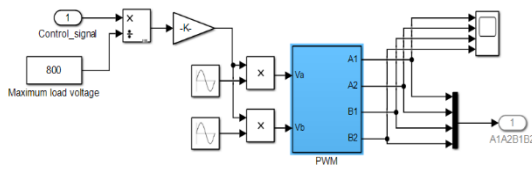


Figure 12: Shows the proposed system implemented on Matlab Simulink.

As show in fig 24 the out Volatge response is related to value of the PWM which generated through the control signal equivalent to temperature. The temperature of the electrode is being adjusted using the PWM technique mentioned earlier. The PWM technique is possible through the aid of microcontroller and the electronic controller circuit connected to the electrode and ESG unit. The PWM with varying temperature is monitored on an oscilloscope, with the plotted signal response being used to increase or decrease the analogue values accordingly. Thus, the PWM, duty cycle and temperature are recorded as shown in Figure 13. For accurate results, the PWM experiment is repeated a number of times and the average values are obtained. The link between PWM and temperature is clearly demonstrated. The temperature (converted to voltage via ADC) is directly proportional to the percentage of duty cycle and the PWM analogue write value. Thus, the temperature and corresponding output voltage both increase with increasing PWM value, with the maximum voltage corresponding to 100% duty cycle. This relationship is plotted in Figure 13 for improved clarity.

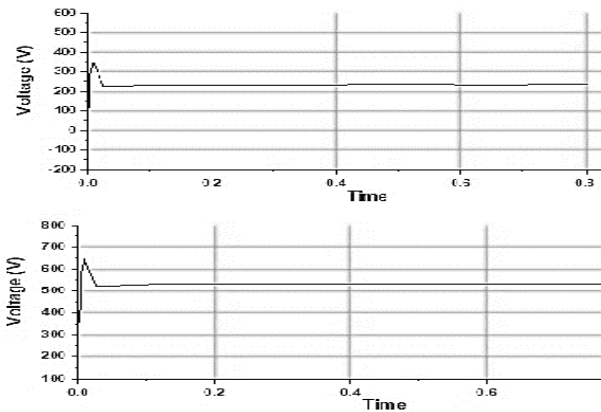


Figure 13 The Volatge output response

The HF inverter is supplied with a duty ratio via the thermal controller shown in Figure 14, where the duty ratio of buck converter is labelled d1is and the duty ratio of the HF inverter is d2. To limit the error between Vref and Vout in voltage mode, the values are compared and sent to a PID compensator. The output is then compared with the HF carrier for conversion to a PWM pulse. To direct the output to select the mode, the output voltage (Vout) and current through the inductor (IL) are measured and compared with the programmed set points. Thus, any of the afore-mentioned modes can be selected according to the controller output.

The system being simulated is the stable and precise dc voltage regulated by the control signal. Hence, the control signal is set to vary from 0V to 5V and an oscilloscope (Tektronix TDS 2002B) with an electrode probe connection is used to monitor the output point and identify the switching power supply output. The output control voltage signal,

which varies according to the set point and feedback signal, is shown in Figure 14. In the Simulation the control signal which would decide the output of the switching power supply was generated according to control signal then the value of the pulse width modulation. when the control signal proportional with PWM signal Simulation diagram is shown in Fig below. The output wave forms of constant power mode are shown in Fig 6.6. Case one when the temperature setpoint at the value 60 C. the in constant current mode, when R1 = 100 ohm, setpoint Output voltage = 100V, Output current= 0.445A and RMS value of output power = 44W as in Fig 6.14. the first diagram represents the PWM value for each of the inverter switch the Output voltage = 100 V.

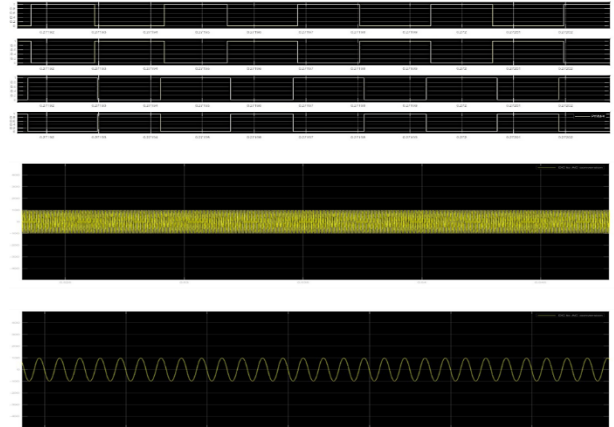


Figure 14:Output signal a- the PWM signal in constant current mode B-the output Volatge waveform C- Maximum Output signal waveform

Now when we increase the setpoint for output temperature at 80 C, then the R = 100 ohm, Output voltage = 200V and output power= 65W and output current is maintained to 0.325A as in Fig 6.7. any change in the input Volatge will not affect the out voltage cause the control signal will correct the output according to setpoint AS Show in fig below the PWM values how it is change according to setpoint.

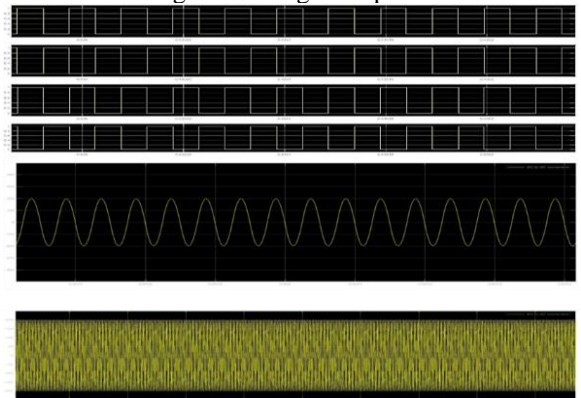


Figure 15: Output signal a- the PWM signal B-the output Volatge waveform C- Maximum Output signal waveform Constant Power Mode

The temperature setting will increase to 100 C when R = 100 ohm, Output voltage = 400V, Output current= 0.2A and RMS value of output power = 80W. as in Fig 6.17. the output Volatge will be increase according to control signal which lead to change in the value of PWM as show in Figure 16 compare with previous setting.

An Experiment on Thermal Damage Prevention via Power Control in Bipolar Electrosurgical Unit

The control signal can be change according to the temperature setting and Volatge setting the switching output Volatge in our case clearly now changing to any change in the setting point.

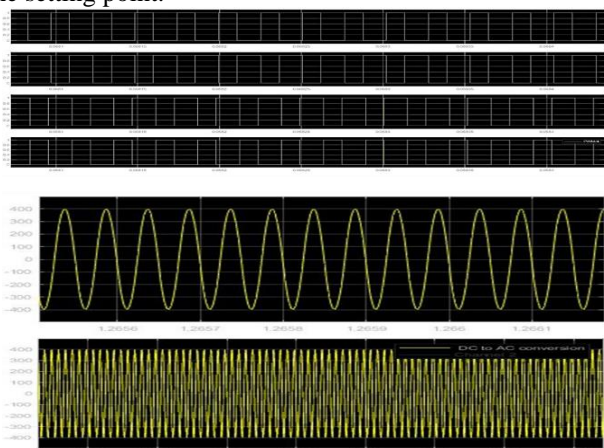


Figure 16: Output signal a- the PWM signal in B-the output Volatge waveform C- Maximum Output signal waveform

This control comprising open and closed loop a high frequency inverter and controller for obtaining regulated power output for electrosurgery [25]. With the increase of setpoint temperature resistance automatic transition between various modes will ensure that voltage and current are maintained within the limits. It also ensures that power variation due to the change in temperature and slow response of the circuit topology to change in impedance is avoided. As a result of which charring of tissues can be eliminated and clinical operations can be made more efficient.

III. SIMULATION VERIFICATION

Following the simulation and analysis of the thermal control system this section verifies it performance through experimental study. Firstly, verification of the operation of the open loop and closed loop system is performed, comparing SIMULINK/MATLAB simulations and experimental waveforms, validating the design. Secondly, production of PWM Signals using open and closed loop system with ESG power supply is conducted. Thirdly, contribution of both system is evaluated, comparing the cutting tissue in both cases.

A. Close Loop verification

Since the clinical effect is determined by the power supplied to the tissue, the proposed ESG prototype is capable of fixing the temperature and controlling the power output of frequently used electrosurgical waveforms. The converter functions in closed loop and the duty cycle is modulated to generate the output current form. According to Yoon et al. (2018), the close loop ESG voltage output and full bridge inverter voltage output on the open circuit are measured using the experimental waveforms shown in Figure 17. These output waveforms were obtained at a load resistance 100 Ω supplied at 100 kHz for duty cycles corresponding to temperatures of 60 °C, 80 °C and 100 °C. The functioning of the closed loop system with a resistive load has been detailed in Section 6.3. The capacity of the controller to rapidly adjust the converter output power in response to changes in the reference temperature was demonstrated in The responses to reference temperature variations of 60, 80 and 100 °C are presented in Figure 17,18,19.

Depending on the tissue type, the load during Electrosurgery can vary between 100 Ω and ~4000 Ω. The capacity of the closed loop system to deliver a self-regulated constant output power while the temperature varies between 60 and 100 °C is indicated in Figure 6.19. According to Munro (2012), when the controller detects a temperature change during an ac output period, a control signal is generated according to specific parameters (e.g. K_i , K_p and K_d) in order to maintain the frequency limit at 100 kHz. While a conventional circuit would take several periods to complete this form of adjustment, the control loop can modify the output current and voltage rapidly in response to the change in load.

These results did not indicate a percentage error during processing of the control system, such that the reading match the set value. The experimental waveforms of an electrode with 100 Ω resistance are frequently used with a duty cycle corresponding to a short duration temperature of up to 60 °C in order to gradually dry out cells and coagulate the tissue. Hence, the setpoint should be 60 °C.

Temperature setting	Temp reading	Duty Cycle	Vin converter	V Out	Power W	I out mA
60	60 C	0.4 %	100 v	100	50 W	0.5

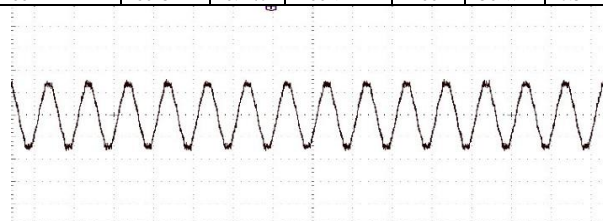


Figure 17 Voltage output and duty cycle at 60C .

As shows in the Figure 18 the open loop waveforms of Electrode at the resistance 100 ohm when the temperature setpoint 80C and the reading value is 80 C and the Volatge output with the duty cycle corresponding waveform used to dry the cells and cut tissue. Also, the Volatge 200 and the output signal 200 V which is mean there is error in the final power produce from the ESG

Temperature setting	Temp reading	Duty Cycle	Vin converter	V Out	Power W	I out mA
80	80 C	0.65%	200 v	200 v	50 W	0.25

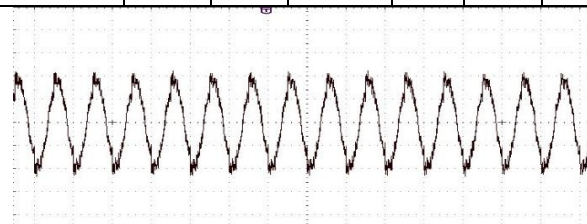


Figure 18 Voltage output and duty cycle at 80C

Finally, we set the temperature value at setpoint 100C still the reading of the temperature show there is no error in reading and the final value can reach to setting point for same duration which is need it for cutting process and that is lead to all the system has no error percentage can lead to less effective process for cutting tissue and can lead to burning by Electrode at the resistance 100 ohm Also, the Volatge 400 and the output signal 400 V which is mean there voltage regulation for ESG. This is illustrated in Figure 19.

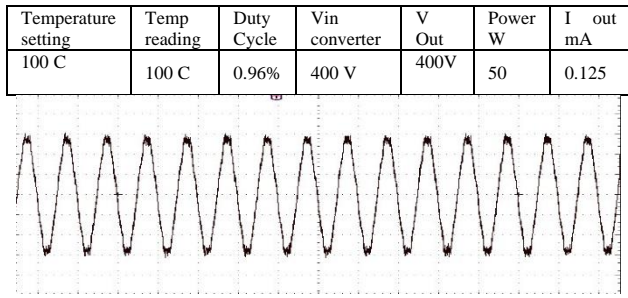


Figure 19 Voltage output and duty cycle at 100C

When the system is closed loop this type of waveform less accurately to 100Ω load as seen in Figure 19. This output type is what would be typical of a resonant converter, and would give surgeons the option to use a familiar output type,

IV. THERMAL DAMAGE MEASUREMENTS

In electrosurgical cutting and tissue coagulation, power regulation is a primary indicator of the extent of thermal spread. While the energy contributes to the cutting speed, tissue damage can result in an increased volume of thermally coagulated tissue. Although Sánchez Trujillo et al. (2016) argue that a degree of thermal coagulation is often necessary for haemostasis, thermal spread need not be regarded as an inevitable outcome of poor output power regulation. Rather, optimal thermal spread can be achieved by increasing the maximum ESG output voltage. An experiment is devised in which the thermal spread is directly measured on test tissue in order to demonstrate the decrease in thermal spread when using enhanced thermal control self-regulation. According to Norris and Maksimovic (2012), chicken tissue is used for testing ESGs because of its highly uniform histological appearance and electrical similarity to human tissue. A cut made in chicken tissue using the ESG electrode using an open-loop generator (i.e. no thermal control) is shown in Figure 20. The absence of voltage-limit and maximum power control during cutting is seen to result in coagulated thermal spread (white areas) and charred tissue (black) around the cut. When the output power exceeds the requisite value, excessive thermal spread leads to unnecessary tissue damage and scarring, thereby hindering the healing process. When the maximum output voltage surpasses the limiting value, tissue charring will result. This is often undesirable as it can obscure the surgical view and lead to unnecessary tissue damage tissue. Hence, failure to precisely regulate the output power, or to provide an adequate method for limiting the voltage, can result in elevated output voltages and undesired charring, or to increased output power and undesired thermal spread. By contrast, Figure 21 demonstrates that effective ESG output regulation is essential for obtaining the desired clinical outcome. Thus, the proposed control scheme can be used to self-regulate the output power during ESG in order to minimise thermal spread by precisely delivering the required power during each cycle. Moreover, the occurrence of undesired tissue charring is limited by the rapid and precise response of the constant voltage mode. These reductions in charring and thermal spread can be expected to result in enhanced surgical outcomes with less scarring and shorter healing periods.

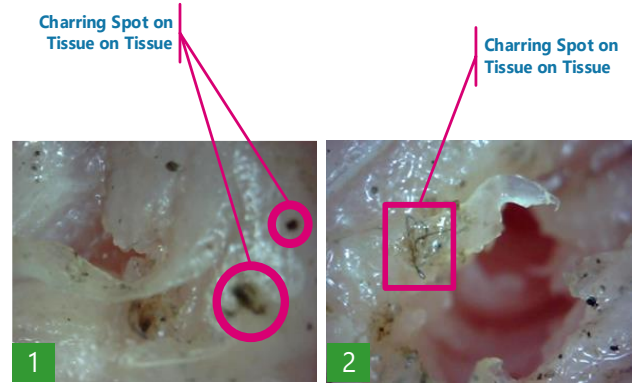


Figure 20 Open loop Tissue Cutting



Figure 21 Closed Loop Tissue Cutting

Figures 20 and 21 clearly show that the laboratory prototype demonstrates significantly decreased thermal spread from either commercially-available unit, as evidenced by decreased volumes of black tissue comparison.

V. CONCLUSION

A prototype ESG is contracted and proposed in this research, that uses a thermal control method in order to create an ideal ESG output characteristic. The high-speed feedback loop results in excellent transient response, with the converter regulating load steps. Voltage- and current-limited modes are invoked equally quickly. Transitions between the two constant-power stages are clean and expedient, and allow constant power source coverage of a full range of load impedances of interest in Monopolar electrosurgery. Experimental results demonstrate that this high-speed control results in excellent output power regulation, with the prototype demonstrating a standard deviation in output power of less than 1 W (compared to ~10 W observed in commercially-available units). tissue analysis of cut chicken tissue proves that output power regulation directly correlates to decreased thermal spread and tissue damage. Thus, this prototype has demonstrated significantly improved clinical effects through the application of high-speed output power regulation. Also notably, compared to prior-art resonant inverter-based designs, the laboratory prototype is a markedly simpler design, as it has no large tank components, and requires only a single current sensor to operate the entire system.



REFERENCES

1. Eggleston, J., et al., *Instant Response™ electrosurgery generator for laparoscopy and endoscopy*. Minimally Invasive Therapy & Allied Technologies, 1997. **6**(5-6): p. 491-495.
2. Charoenkwan, K., et al., *Scalpel versus electrosurgery for major abdominal incisions*. Cochrane Database of Systematic Reviews, 2017(6).
3. Taheri, A., et al., *Electrosurgery: part I. Basics and principles*. Journal of the American Academy of Dermatology, 2014. **70**(4): p. 591. e1-591. e14.
4. Grassi, E. and K. Tsakalis, *PID controller tuning by frequency loop-shaping: application to diffusion furnace temperature control*. IEEE Transactions on Control Systems Technology, 2000. **8**(5): p. 842-847.
5. Åström, K.J., T. Häggglund, and K.J. Astrom, *Advanced PID control*. 2006.
6. Gibbs, R., et al., *Portable temperature control system*. 1999, Google Patents.
7. Thomas, P.A., et al., *Cytomorphologic characteristics of thermal injury related to endocervical brushing following loop electrosurgical excision procedure (LEEP)*. Diagnostic cytopathology, 1996. **14**(3): p. 212-215.
8. Bishoff, J.T., et al., *Laparoscopic bowel injury: incidence and clinical presentation*. The Journal of urology, 1999. **161**(3): p. 887-890.
9. Ata, A.H., et al., *Distal thermal injury from monopolar electrosurgery*. Surgical laparoscopy & endoscopy, 1993. **3**(4): p. 323-327.
10. Truckai, C., et al., *Electrosurgical jaw structure for controlled energy delivery*. 2005, Google Patents.
11. McLyman, C.W.T., *Transformer and inductor design handbook*, M.O. Thurston, Editor. 2004.
12. Liang, T.-J. and K. Tseng, *Analysis of integrated boost-flyback step-up converter*. IEE Proceedings-Electric Power Applications, 2005. **152**(2): p. 217-225.
13. Erickson, R., M. Madigan, and S. Singer. *Design of a simple high-power-factor rectifier based on the flyback converter*. in *IEEE Applied Power Electronics Conference*. 1990.
14. J. Sun, *Pulse-Width Modulation*, in *Dynamics and Control of Switched Electronic Systems*. 2012.
15. Meynard, T. and H. Foch. *Multi-level conversion: high voltage choppers and voltage-source inverters*. in *Power Electronics Specialists Conference, 1992. PESC'92 Record., 23rd Annual IEEE*. 1992. IEEE.
16. Hernandez, A.F. and G.W. Bruning, *High frequency inverter with power-line-controlled frequency modulation*. 1995, Google Patents.
17. Farin, G. and P. Putz, *High-frequency electrosurgical unit with timed safety shut down interlock*. 1987, Google Patents.
18. Kliccek, M.S., *Automatic control for energy from an electrosurgical generator*. 2001, Google Patents.
19. Swanson, D.K., J.G. Wayne, and D. Panescu, *Systems and methods for controlling power in an electrosurgical probe*. 2002, Google Patents.
20. Thompson, R., *Electrosurgical generator and method with voltage and frequency regulated high-voltage current mode power supply*. 2005, Google Patents.
21. Dodde, R.E., et al., *Monopolar electrosurgical thermal management for minimizing tissue damage*. IEEE Transactions on biomedical engineering, 2012. **59**(1): p. 167-173.
22. Oosten, R.L., *Electrosurgical generator*. 1983, Google Patents.
23. Wham, R.H., T.A. Sturm, and W.D. Faulkner, *Method and system for programming and controlling an electrosurgical generator system*. 2012, Google Patents.
24. Swanson, D.K., et al., *Systems and methods for controlling power in an electrosurgical probe*. 2002, Google Patents.
25. Jensen, S. and D. Maksimovic, *Fast tracking electrosurgical generator using two-rail multiphase buck converter with gan switches*. IEEE Transactions on Power Electronics, 2017. **32**(1): p. 634-641.

AUTHORS PROFILE



Ali Idham Alzaidi received his B.Eng. degree in Biomedical Engineering from North Technical University of Mosul, Iraq, in 2000 and M.Sc. in Biomedical Engineering from University of Bridgeport, USA, in 2011. He is currently with the School of Biomedical Engineering, Universiti Teknologi Malaysia. His research interests include Electrosurgical System, MATLAB, Switch Mode Power Supply, and Thermal Control.



Mohammad Rava received his B.Sc. degree in Information Technology, and then followed it through with a M.Eng in Software Engineering, both obtained in the Assumption University from Thailand. His PhD was undertaken in Universiti Teknologi Malaysia in the school of computing with a focus on Software Engineering. His research interests are in Artificial Intelligence oriented topics such as Machine Learning, and Metaheuristic Algorithms, as well as the use of AI in other fields such as Biochemistry and Chemical Engineering.



Azli Yahya Azli Yahya received his B.Eng. (Hons.) degree in Electro-Mechanical Power System and M.Sc. degree in Electronic Production from University of Glamorgan, Wales, UK. In 2006, he obtained his PhD degree in Electronic/Electrical Engineering from University of Loughborough, UK. He is currently an Associate Professor at School of Biomedical Engineering and Health Sciences, Faculty of Engineering, Universiti Teknologi Malaysia. His research areas cover Electrical Discharge Machining System, Analog/Digital Circuit, Microcontroller, PSPICE, MATLAB, Switch Mode Power Supply, Biomedical Instrumentation.